

Digital Single Lens Reflex Photometry in White Light: a New Concept Tested on Data from the High Amplitude δ Scuti Star V703 Scorpii

Roy Andrew Axelsen

P.O. Box 706, Kenmore, Queensland 4069, Australia; reaxelsen@gmail.com

Received November 21, 2016; revised March 19, 2017; accepted March 22, 2017

Abstract A novel method of digital single lens reflex (DSLR) photometry is described. It derives non-transformed instrumental magnitudes from white light (green, blue, and red channels of the DSLR sensor combined), and is assessed by comparing the results with non-transformed instrumental magnitudes from the green channel alone, and with green channel magnitudes transformed to the Johnson V standard. The white light data and the non-transformed green channel data allow differential photometry only; true magnitude values cannot be calculated. The same time series images of the high amplitude δ Scuti star V703 Scorpii were processed by all three methods. The light curves from the white light data were almost identical to those from the non-transformed green channel data and to those in V magnitude, but with a slightly greater amplitude for the variable star (from highest peak to lowest trough of the light curve on each night) in the white light curves. There was also an impression, in some areas, of slightly smoother curves from the white light data, implying improved precision. The check star data in white light showed slightly smaller ranges and standard deviations for most nights, and for all nights averaged, than those for the non-transformed green channel data, and for the transformed V magnitude data, implying that the best precision was achieved by using the data in white light. For most of the peaks in the light curve, the times of maximum in white light differed little from those in V magnitude. Fourier analysis using the Lomb-Scargle method revealed identical power spectra and identical discovered frequencies in white light and in V magnitude. DSLR photometry in white light is a valid procedure, at least in those cases where the color indices of the variable and comparison stars differ by only small values. It is considered promising for the timing of maxima and minima of light curves and for Fourier analysis of those stars with more than one period.

1. Introduction

Following the ground breaking work of Hoot (2007) and Loughney (2010), amateur astronomers have used DSLR cameras to make significant contributions to variable star photometry (Kloppenborg *et al.* 2012; Richards 2012; Axelsen 2014a–2014d, 2015; Axelsen and Napier Munn 2015, 2016; Deshmukh 2015; Walker *et al.* 2015). The AAVSO provides detailed methods for observers who wish to avail themselves of this technique, which is capable of yielding results with high precision using modest equipment (AAVSO 2016).

Aperture photometry on images from a DSLR camera must take account of the fact that the camera sensor is composed of a color filter array (Bayer matrix) of green, blue, and red elements. The processing of images from one of the three color channels, usually the green channel, provides the opportunity for simple differential photometry to study events such as the timing of maxima of light curves of pulsating variable stars, and the timing of eclipses in binary stellar systems. In such cases, it is not necessary to transform the magnitude data to a standard system. For more stringent work, photometry of images from two channels (green and blue, for example) or all three channels does allow transformation of the results to a standard system (AAVSO 2016).

One of the disadvantages of photometry with a DSLR camera in comparison with CCD photometry is that not all of the pixels of the DSLR sensor are used, as the green-, blue-, and red-filtered pixels comprise 50%, 25%, and 25%, respectively, of the surface of the sensor. For photometry based on the green channel, 50% of the light reaching the sensor therefore cannot be used, and for each of the blue and red channels, the proportion of unused pixels increases to 75%.

In view of these disadvantages, it was decided to trial differential photometry with a DSLR camera using all of the light reaching the sensor, by processing images containing data from all three color channels simultaneously (i.e., images in white light). To the author's knowledge, this strategy has not previously been used. The high amplitude δ Scuti star V703 Scorpii was chosen as a test case for the procedure. It is accepted by most authors to have two periods, 0.11521803 d and 0.14996 d (Plaut 1948 quoted in Ponsen 1963; Ponsen 1961, 1963; Oosterhoff 1966; Koen 2001). Two different sets of measures were used to compare the performance of white light DSLR photometry with differential photometry using non-transformed magnitudes from the green channel, and photometric data transformed to the Johnson V standard; the amplitude of the light curve of V703 Sco in magnitude units, measured from the lowest trough to the highest peak each night; and the standard deviation of the check star magnitudes from each night's time series data. A further two sets of measures applied to the variable star data were used to compare the performance of white light DSLR with photometric data transformed to the Johnson V system; Fourier analysis to identify pulsation frequencies; and the determination of the times of maximum of the peaks of the light curve.

2. Data and analysis

2.1. Observations

V703 Sco was observed by DSLR photometry over 12 nights in 2016 from 11 May to 1 July. A total of 1,254 magnitude determinations were obtained from a total observing time of 62.78 hours. The minimum number of observations on one night was 88, over 4.41 hours, and the maximum number was

123, over 6.19 hours. The target field was imaged mostly to the east of the meridian, and for a short time after transit. No meridian flips were performed because incremental shifts in magnitude values were seen after meridian flips when V703 Sco was studied in the 2014 season.

RAW images were taken with a Canon EOS 500D DSLR camera through an 80-mm refracting telescope with a focal length of 600mm on a Losmandy GM8 German equatorial mount. Exposures of 170 seconds were made at ISO 400, at intervals of 180 seconds (i.e., one image was taken every 180 seconds). Dark frames were taken after the completion of light frames. Flat fields were captured near sunrise the following morning through a white acrylic sheet placed over the front of the telescope, which was aimed at the zenith.

2.2. Data reduction

Aperture photometry was performed with the software AIP4WIN version 2.4.0 (Berry and Burnell 2011). Measurements from the green channel enabled the calculation of non-transformed differential magnitudes from the formulae:

$$\text{Var } g - \text{Comp } g \tag{1}$$

$$\text{Chk } g - \text{Comp } g \tag{2}$$

where *g* is the instrumental magnitude and *Var*, *Comp*, and *Chk* refer to the variable, comparison, and check stars, respectively. Measurements from the green and blue channels were used to calculate magnitudes transformed to the Johnson *V* system, employing transformation coefficients determined from standard stars in the E regions (Menzies *et al.* 1989). For white light differential photometry, the settings in AIP4WIN were as follows. In *Preferences > DSLR Conversion Settings > DeBayer, Convert Color to Grayscale*, the red, green, and blue scales were all set to 1.0 simultaneously. Differential magnitudes for white light photometry were calculated from the formulae:

$$\text{Var } wl - \text{Comp } wl \tag{3}$$

$$\text{Chk } wl - \text{Comp } wl \tag{4}$$

where *wl* is the white light instrumental magnitude and *Var*, *Comp*, and *Chk* refer to the variable, comparison, and check stars respectively.

The comparison and check stars were HD 160927 and HD 160432, respectively. The *V* magnitude and *B–V* color index for the comparison star were taken to be 8.727 and 0.533, respectively, and the corresponding values for the check star were taken to be 9.159 and 0.457. These two stars were chosen because their *B–V* color indices are close to that of V703 Sco, which from the author’s photometry varies from 0.2 to 0.5 approximately.

The time in JD of each magnitude calculation was taken to be the mid point of each DSLR exposure. The heliocentric correction for each night’s data was calculated for the mid point in time of the observing run for the night, and the correction applied to all data points for that night. Fourier analyses and

the determination of the times of maximum of the light curve used the heliocentric data.

2.3. Time series analysis and determination of the times of maximum of the variable star light curve

The software PERANSO (Vanmuster 2014) was used. Fourier analysis employed the Lomb-Scargle routine. The times of maximum of the light curve were taken as the maximum values of fifth order polynomial functions fitted to the magnitude values around each peak in the light curve.

3. Results

3.1. Metrics of the light curves of V703 Sco and the check star

Light curves from two representative nights are shown in Figures 1 and 2, respectively. In each figure, the top panel shows transformed *V* magnitudes (hereafter referred to simply as “*V* magnitudes”), the middle panel shows non-transformed differential magnitudes from the green channel (hereafter referred to simply as “green magnitudes”), and the bottom panel shows differential magnitudes in white light (hereafter referred to simply as “white light magnitudes”). Each light curve shows data both for the variable star and the check star, with the check star magnitudes represented as the calculated magnitudes minus 1.3 so that variable and check star data can both be seen optimally. The variation in the amplitude between adjacent peaks in the light curves of V703 Sco is typical of a variable star with more than one period.

The variable star light curves in Figure 1, from 11 May 2016, show peaks 1 and 2 (labelled in the top panel of the figure), corresponding to the numbers of the peaks in the first column of Tables 3 and 4. Figure 2, from 13 May 2016, shows peak 4 (labelled in the top panel of the figure), with the latter

Table 1. Photometric data for V703 Sco, listing transformed *V* magnitudes, non-transformed differential magnitudes from the green channel, and differential magnitudes in white light.

<i>Date</i> (2016)	<i>Var V</i> <i>Range</i>	<i>Var g</i> <i>Range</i>	<i>Var wl</i> <i>Range</i>	<i>Var g, Var V</i> <i>Δ Range</i>	<i>Var wl, Var V</i> <i>Δ Range</i>
May–11	0.479	0.496	0.506	0.017	0.027
May–12	0.469	0.486	0.491	0.017	0.022
May–13	0.483	0.500	0.516	0.017	0.033
May–14	0.482	0.498	0.509	0.016	0.027
Jun–08	0.461	0.469	0.474	0.008	0.013
Jun–09	0.471	0.489	0.503	0.018	0.032
Jun–10	0.488	0.503	0.516	0.015	0.028
Jun–25	0.414	0.428	0.440	0.014	0.026
Jun–27	0.475	0.489	0.490	0.014	0.015
Jun–28	0.390	0.402	0.407	0.012	0.017
Jun–29	0.454	0.469	0.476	0.015	0.022
Jul–01	0.353	0.366	0.374	0.013	0.021
Mean	0.452	0.466	0.475	0.015	0.024
SD	0.043	0.044	0.046	0.003	0.006

Notes. Abbreviations in the above table: *Var* = Variable star; *V* = Transformed *V* magnitude photometric data; *Range* = Difference between the maximum and minimum magnitudes for each night; *g* = Non-transformed differential magnitudes from the green channel; *wl* = White light non-transformed differential magnitudes from all three channels; *Δ Range* = Difference between the two ranges as indicated at the head of each column; *SD* = Standard deviation.

Table 2. Photometric data for the check star, listing transformed V magnitudes, non-transformed differential magnitudes from the green channel, and differential magnitudes in white light.

<i>Date</i> (2016)	<i>Chk V</i> <i>Range</i>	<i>Chk g</i> <i>Range</i>	<i>Chk wl</i> <i>Range</i>	<i>Chk g, Chk V</i> <i>Δ Range</i>	<i>Chk wl, Chk V</i> <i>Δ Range</i>	<i>Chk V</i> <i>SD</i>	<i>Chk g</i> <i>SD</i>	<i>Chk wl</i> <i>SD</i>
May-11	0.082	0.067	0.060	-0.015	-0.022	0.014	0.012	0.010
May-12	0.068	0.064	0.053	-0.004	-0.015	0.013	0.011	0.009
May-13	0.105	0.079	0.056	-0.026	-0.049	0.016	0.012	0.010
May-14	0.054	0.061	0.047	0.007	-0.007	0.011	0.009	0.007
Jun-08	0.092	0.065	0.048	-0.027	-0.044	0.011	0.009	0.007
Jun-09	0.088	0.075	0.078	-0.013	-0.010	0.015	0.013	0.012
Jun-10	0.183	0.151	0.129	-0.032	-0.054	0.018	0.016	0.014
Jun-25	0.043	0.033	0.042	-0.010	-0.001	0.009	0.007	0.007
Jun-27	0.058	0.052	0.048	-0.006	-0.010	0.011	0.010	0.009
Jun-28	0.039	0.031	0.031	-0.008	-0.008	0.008	0.006	0.006
Jun-29	0.046	0.040	0.037	-0.006	-0.009	0.010	0.008	0.007
Jul-01	0.036	0.035	0.033	-0.001	-0.003	0.008	0.007	0.006
Mean	0.075	0.063	0.055	-0.012	-0.019	0.012	0.010	0.009
SD	0.041	0.032	0.027	0.012	0.019	0.003	0.003	0.002

Notes. Abbreviations in the above table: *Chk* = Check star; *V, Range, g, wl, Δ Range* and *SD* are as for the Notes to Table 1.

being one of the two peaks for which the time of maximum light differed by an unacceptably large value between V magnitude data and white light magnitude data (see below).

The light curves showing magnitudes in white light are similar to those showing green magnitudes and V magnitudes, but there is an impression of slightly smoother areas in the curves for the variable star in the white light panels. Columns 2, 3, and 4 of Table 1 show the data for the amplitudes of the V703 Sco light curves for each night and averaged over all nights. The amplitudes of the variable star light curves from the three different photometric methods show very little difference, with the greatest being on average only 0.024 magnitude units, between the light curves in white light and the light curves in V magnitude.

The check star light curves show poor precision during the early part of each night, when the airmass was 4.2 on 11 May 2016 (Figure 1) and 3.8 on 13 May 2016 (Figure 2). The precision improves later in the night, as the altitude of the star increases and the air mass decreases. There is an impression that the variance is better for the green magnitude data than for the V-magnitude data, and better again for the white light data. These impressions are confirmed by the analysis of the numerical values shown in Table 2, which are considered in detail in the following paragraph.

Columns 2, 3, and 4 list the ranges in magnitude units of the observations for the check star for each night, and at the bottom of the table, the means and standard deviations for all nights. For each observing night, the range is slightly less for the green magnitude data than for the data in V magnitude. For most observing nights, the range for the white light magnitude is less again. The means and standard deviations of the magnitude ranges for the check star show that the most precise data are those for white light magnitudes, and the least precise the V magnitudes, although the differences are small. Columns 7, 8, and 9 analyze the standard deviation of the magnitude values for each night, and their averages. The differences are again small, but once more the white light data are more precise than those for the other two methods of magnitude calculation.

The times of maximum (TOM) of all peaks with long ascending and long descending limbs are shown in Table 3. Peaks associated with a short ascending or descending limb were not measured. The times were determined in PERANSO as the maximum values of fifth-order polynomial expressions fitted to the peaks of the light curve. After this was done for the white light data and the V magnitude data, the difference between the TOM for white light and V magnitude was calculated for each peak, using the formula: TOM in white light minus TOM in V magnitude. All but two of the differences lay within a range of 2.30 min. (from -1.44 min. to 0.86 min.), whereas the other two differences were -6.38 min. and 8.80 min. Those results which lay within a range of 2.30 min. were considered acceptable, because they compared favourably with results in the author's previous DSLR photometric study of ZZ Mic (Axelsen 2015) in which the O-C values for 14 TOM obtained over a span of 9.3 days lay within a range of 2.62 min. The other two results (-6.38 min. and 8.80 min.) were therefore considered to be unacceptable. Figure 3 shows part of the light curve of V703 Sco, representing the region around peak 4 (as listed in Tables 3 and 4) plotted in PERANSO, with a fitted fifth-order polynomial expression. The upper panel is the light curve in V magnitude, and the lower panel the light curve from white light magnitude data. The white light plot is smoother than the V magnitude plot.

In view of the two unacceptable results, the TOM for all of the peaks were recalculated from the light curve data, but using center moving averages across three data points instead of the individual magnitude determinations. The results are shown in Table 4. Again, peaks 4 and 10 show unacceptably large differences between the white light and V magnitude data.

The TOM of the two peaks giving the discrepant results were remeasured using the Podgson method (Percy 2007), which involved printing the parts of the light curve containing the peaks to be measured and drawing by hand a smooth curve through the data. Several equally spaced horizontal chords are then drawn between the ascending and descending limbs of the light curve, and the mid points of the chords marked. A smooth

Table 3. Times of maximum (TOM) of V703 Sco in heliocentric Julian days (HJD) in white light (wl) and V magnitude.

Peak	HJD TOM wl	Error	HJD TOM V Mag	Error	wl TOM – V Mag TOM (d)	wl TOM – V Mag TOM (min)
1	2457520.0102	0.0010	2457520.0102	0.0012	0.0	-0.01
2	2457520.1309	0.0007	2457520.1310	0.0007	-0.0001	-0.14
3	2457521.0485	0.0009	2457521.0489	0.0013	-0.0004	-0.58
4	2457522.0822	0.0007	2457522.0866	0.0091	-0.0044	-6.34
5	2457523.0059	0.0008	2457523.0069	0.0008	-0.0010	-1.44
6	2457523.1278	0.0005	2457523.1278	0.0009	0.0	0.0
7	2457548.0171	0.0008	2457548.0169	0.0010	0.0002	0.29
8	2457548.9330	0.0010	2457548.9331	0.0013	-0.0001	-0.14
9	2457549.0592	0.0010	2457549.0590	0.0012	0.0002	0.29
10	2457549.9725	0.0007	2457549.9664	0.0009	0.0061	8.78
11	2457564.9573	0.0008	2457564.9569	0.0008	0.0004	0.58
12	2457566.9124	0.0011	2457566.9127	0.0010	-0.0003	-0.43
13	2457567.9544	0.0011	2457567.9538	0.0011	0.0006	0.86
14	2457568.9956	0.0009	2457568.9959	0.0014	-0.0003	-0.43
15	2457570.9520	0.0012	2457570.9516	0.0013	0.0004	0.58

Notes: The TOM were determined in PERANSO using a 5th order polynomial expression fitted to the peaks of the light curve. The last two columns on the right show the differences in days (d) and minutes (min) between the TOM in wl and the TOM in V magnitude. Unacceptably large differences are seen for peak 4 and peak 10.

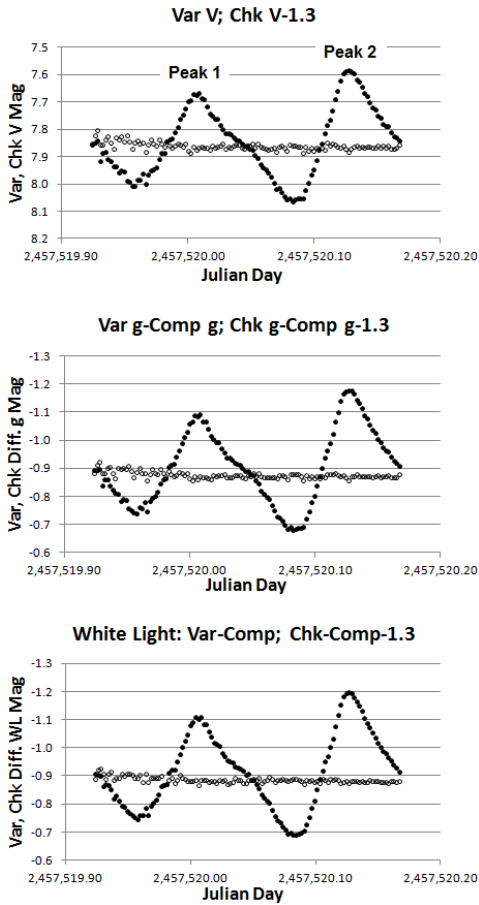


Figure 1. Light curves of V703 Sco and the check star from observations taken on one night and showing Peaks 1 and 2 (as listed in Tables 3 and 4). The check star magnitudes shown are the actual calculated magnitudes minus 1.3. The upper panel shows magnitudes transformed to the Johnson V system. The middle panel shows non-transformed magnitudes from the green channel data. The bottom panel shows non-transformed magnitudes from white light images.

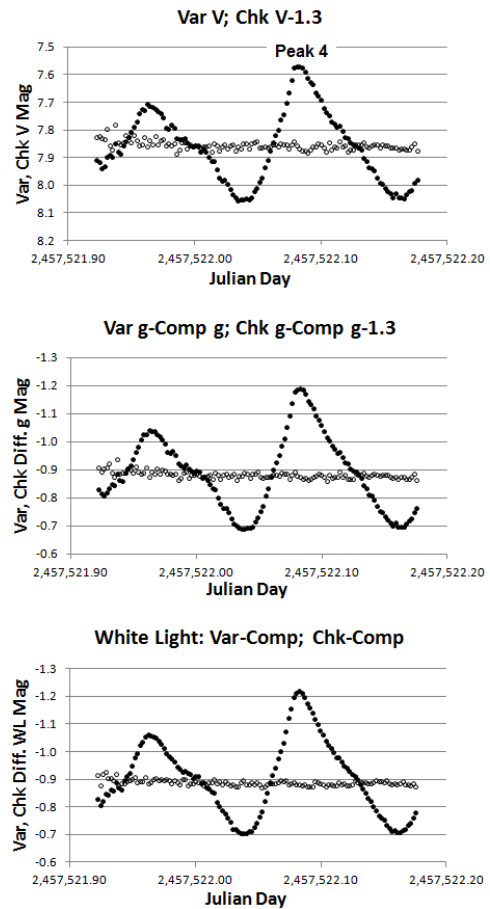


Figure 2. Light curves of V703 Sco and the check star from observations taken on one night and including Peak 4 (as listed in Tables 3 and 4).

Table 4. Times of maximum (TOM) of V703 Sco from center moving averages (over 3 magnitude determinations), in heliocentric Julian days (HJD) in white light (wl) and V magnitude.

Peak	HJD TOM wl	Error	HJD TOM V Mag	Error	wl TOM – V Mag TOM (d)	wl TOM – V Mag TOM (min)
1	2457520.0105	0.0006	2457520.0112	0.0007	-0.0007	-1.01
2	2457520.1310	0.0004	2457520.1312	0.0004	-0.0002	-0.29
3	2457521.0486	0.0005	2457521.0487	0.0006	-0.0001	-0.14
4	2457522.0824	0.0004	2457522.0868	0.0005	-0.0044	-6.34
5	2457523.0061	0.0005	2457523.0067	0.0004	-0.0006	-0.86
6	2457523.1279	0.0003	2457523.1279	0.0006	0.0	0.00
7	2457548.0173	0.0005	2457548.0172	0.0006	0.0001	0.14
8	2457548.9325	0.0006	2457548.9323	0.0006	0.0002	0.29
9	2457549.0590	0.0005	2457549.0591	0.0007	-0.0001	-0.14
10	2457549.9728	0.0006	2457549.9669	0.0007	0.0059	8.50
11	2457564.9574	0.0006	2457564.9573	0.0006	0.0001	0.14
12	2457566.9123	0.0006	2457566.9127	0.0006	-0.0004	-0.58
13	2457567.9544	0.0007	2457567.9538	0.0006	0.0006	0.86
14	2457568.9954	0.0005	2457568.9954	0.0006	0.0	0.00
15	2457570.9520	0.0005	2457570.9519	0.0008	0.0001	0.14

Notes: The TOM were determined in PERANSO using a 5th order polynomial expression fitted to the peaks of the light curve. The last two columns on the right show the differences in days (d) and minutes (min) between the TOM in wl and the TOM in V magnitude. Unacceptably large differences are seen for peak 4 and peak 10.

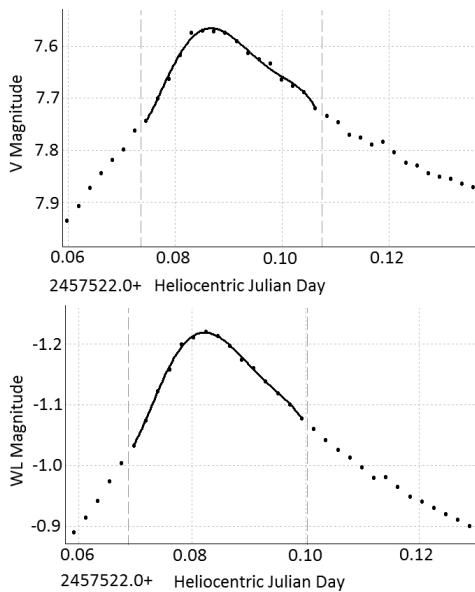


Figure 3. Part of the light curve of V703 Sco, comprising the region around Peak 4 (as listed in Tables 3 and 4). This is one of the peaks where the TOM differed markedly between the V magnitude data (top panel) and white light magnitude data (bottom panel). The curves were fitted in PERANSO as 5th order polynomial expressions. The Peak and the descending limb of the light curve in white light are smoother than those in the V magnitude light curve.

line is then drawn by hand through the mid points of the chords, and the point at which that line intersects the light curve is taken to be the TOM of the peak. The results for this procedure are shown in Table 5, which reveals that the large discrepancies between the white light TOM and the V magnitude TOM, as seen in Tables 1 and 2, did not persist.

3.2. Fourier analysis of the light curve of V703 Sco in V magnitude and in white light

The Lomb-Scargle routine in the software PERANSO was employed for this analysis which was applied to the

V-magnitude data and the data in white light, with identical results. Each frequency search requires the input of the start and end frequencies and the resolution, i.e., the number of steps between those frequencies. For f1 (the first frequency sought), start and end frequencies initially selected were 0 and 20 cd^{-1} with a resolution of 800, yielding a dominant frequency of 8.67783 cd^{-1} . This frequency was refined by a second search between 8.5 and 8.8 cd^{-1} with a resolution of 1,000, the new frequency being 8.67760 cd^{-1} . In each case, the corresponding period to four decimal places was 0.1152 d. The data were then prewhitened for the refined frequency, and f2 (the second frequency sought) was found between start and end frequencies of 0 and 20 cd^{-1} with a resolution of 750, yielding a frequency of 6.67333 cd^{-1} . This frequency was refined by a second search between 6 and 7 cd^{-1} with a resolution of 1,000, yielding a frequency of 6.66900 cd^{-1} . In each case the corresponding period to four decimal places was 0.1499 d. The power spectra from these analyses for the light curve in white light are shown in Figure 4. As the power spectra for the V-magnitude light curve were identical, they are not shown. The two periods, 0.1152 d and 0.1499 d, are identical (to four decimal places) to those reported in the previous literature.

4. Discussion

The purpose of this study was to determine whether or not DSLR photometry in white light yielded valid data by comparing the results with photometry based on non-transformed data from the green channel of the DSLR sensor, and with photometry based on data from the green channel transformed to the Johnson V standard. Because only simple differential photometry could be achieved from the non-transformed data from the green channel and from white light data, no useful information about the color of the variable star could be gained. Therefore, analyses of the results were confined to parameters involving time, namely, the times of maximum of the light curve and period analysis using Fourier

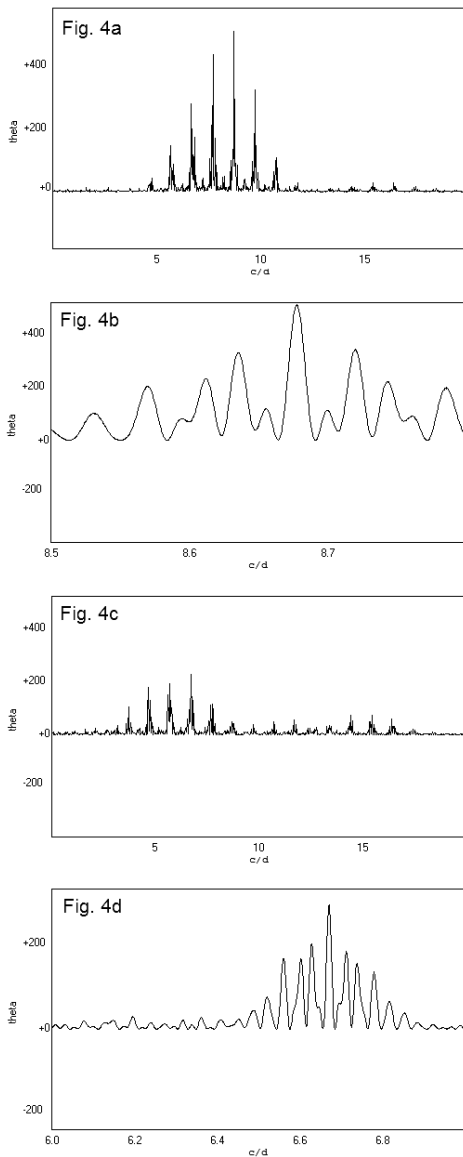


Figure 4. PERANSO Lomb-Scargle power spectra of V703 Sco from white light images. The power spectra of V magnitude data were identical, and are not shown. In the following, f1 is the first discovered frequency and P1 its corresponding period; f2 is the second discovered frequency and P2 its corresponding period. 4a: f1=8.67783 c d-1, P1=0.1152 d, from 0-20 c d-1 at a resolution of 800. 4b: refined frequency for f1=8.6770 c d-1, P1=0.1152, from 8.5-8.8 c d-1 at a resolution of 1000. 4c: after prewhitening for 8.6770 c d-1, f2=6.67333 c d-1, P2=0.1499 d, from 0-20 c d-1 at a resolution of 750. 4d: refined frequency for f2=6.66900 c d-1, P2=0.1499 d, from 6-7 c d-1 at a resolution of 1000.

Table 5. Times of maximum (TOM) of peaks 4 and 10 (from Tables 3 and 4 above) of the light curve of V703 Sco, remeasured by the Podgson method (see text of paper).

Peak	HJD TOM wl	HJD TOM V Mag	wlTOM-VMag TOM (d)	wlTOM-VMag TOM (min)
4	2457522.082	2457522.081	0.001	1.44
10	2457549.966	2457549.966	0.0	0.0

Note: Abbreviations are as for Table 4.

decomposition. The amplitudes of the light curves for each night, and the ranges and standard deviations of the check star magnitude data for each night were also compared between transformed V magnitude data, non-transformed data from the green channel, and white light data.

When the TOM of the light curve were determined by fitting fifth-order polynomial expressions to the peaks, 13 of the 15 measured peaks gave similar results in white light and V magnitude, with the largest difference being 2.30 min. However, peaks 4 and 10 (from Table 1) had discrepancies of -6.34 min and 8.78 min, respectively, between the white light and V magnitude times, which are too large to be acceptable. In view of these results, the TOM were recalculated from light curve data plotted as center moving averages over three consecutive magnitude values. As in the case of the non-averaged magnitude data large discrepancies between white light and V magnitude TOM were still present for peaks 4 and 10, whereas all of the other peaks had acceptable results (Table 3).

It was considered likely that the large discrepancies between TOM were based upon imprecision in the magnitude determinations near the peaks of the light curve, resulting in spurious assignment of the TOM based on the fitting of the fifth-order polynomial expressions in PERANSO. Therefore, the TOM of the peaks with the discrepant results for the raw magnitude data (not the moving average data) were recalculated using the Podgson method of bisected chords, a manual method requiring the use of curve fitting by hand. With the latter, the discrepancies between white light and V magnitude TOM became much less, the largest now being 1.44 min.

In order to set these results in the context of other studies which have published the TOM of light curves for the construction of O-C (observed minus computed) diagrams of variable stars, the author's previously published work on the δ Scuti star ZZ Mic is considered. The range of O-C values calculated from observations taken over a time of 9.3 d was 2.62 min. (Axelsen and Napier-Munn 2015). It is therefore concluded that the precision of the determination of TOM of light curve peaks from white light photometry would be sufficient for successful application to the study of variable stars using O-C diagrams. However, in view of the unacceptably large differences between the TOM of white light and V magnitude data for 2 of 15 light curve peaks for V703 Sco, caution is required in the use of white light DSLR photometry. If this method is used for O-C diagrams, it would be necessary to gather TOM data from several peaks over relatively short periods of time to ensure that the variance of the data is acceptable.

The final test was to compare results of Fourier analysis of V703 Sco white light data with the results of a similar analysis of data in V magnitude. The comparison clearly showed that the analyses were identical in all respects: the appearances of the power spectra, the dominant frequencies revealed before and after refining the frequency searches, and the outcome of a second frequency search after prewhitening for the first frequency. It is concluded that it is valid to carry out Fourier analysis of DSLR photometric data taken in white light.

Finally, it is necessary to consider the colors of the variable, comparison, and check stars used in this study. The B-V for

V703 Sco varies from 0.2 to 0.5 from the author's DSLR photometry in B and V. The B–V color indices of the comparison and check stars (HD 160927 and HD 160432) were 0.533 and 0.457, respectively. The latter two values are relatively close to the range of B–V values displayed by V703 Sco as it cycles through a period. Therefore, if DSLR photometry in white light is to be attempted with variable and comparison stars having markedly differing colors and thus markedly differing B–V color indices, caution should be observed in the interpretation of the results, as it should not be assumed that the precision of the measurements would be similar to the precision described in the present paper.

5. Conclusions

A novel technique of DSLR photometry, involving analyzing images in white light, has been investigated using data obtained from a study of the high amplitude δ Scuti star V703 Sco. Images in white light can be used only to analyze variable star parameters involving time. Aperture photometry was performed on images taken in white light, and repeated on the same set of images to obtain non-transformed differential magnitudes from the green channel, and magnitudes transformed to the Johnson V system. Analysis indicates that the precision of white light photometry is slightly greater than the precision of photometry with non-transformed green channel data, and slightly greater than the precision of measurements in V magnitude. For the majority of peaks, the TOM of the light curves in white light and V magnitude differed by only small time intervals. Fourier analysis by the Lomb-Scargle method showed identical results for white light data and data in V magnitude. It is concluded that DSLR photometry of variable stars in white light is a valid technique for timing the peaks (and by inference the troughs) of light curves, and for Fourier analysis of pulsating variable stars, at least for variable and comparison stars having similar color indices.

References

- AAVSO. 2016, *The AAVSO DSLR Observing Manual, Version 1.4*, AAVSO, Cambridge, MA (<https://www.aavso.org/dslr-observing-manual>).
- Axelsen, R. A. 2014a, *J. Amer. Assoc. Var. Star Obs.*, **42**, 37.
- Axelsen, R. A. 2014b, *J. Amer. Assoc. Var. Star Obs.*, **42**, 44.
- Axelsen, R. A. 2014c, *J. Amer. Assoc. Var. Star Obs.*, **42**, 287.
- Axelsen, R. A. 2014d, *J. Amer. Assoc. Var. Star Obs.*, **42**, 292.
- Axelsen, R. A. 2015, *J. Amer. Assoc. Var. Star Obs.*, **43**, 182.
- Axelsen, R. A., and Napier-Munn, T. 2015, *J. Amer. Assoc. Var. Star Obs.*, **43**, 50.
- Axelsen, R. A., and Napier-Munn, T. 2016, *J. Amer. Assoc. Var. Star Obs.*, **44**, 119.
- Berry, R., and Burnell, J. 2011, "Astronomical Image Processing for Windows," version 2.4.0, provided with *The Handbook of Astronomical Image Processing*, Willmann-Bell, Richmond, VA.
- Deshmukh, S. 2015, *J. Amer. Assoc. Var. Star Obs.*, **43**, 172.
- Hoot, J. E. 2007, in *The Society for Astronomical Sciences 26th Annual Symposium on Telescope Science*, Society for Astronomical Sciences, Rancho Cucamonga, CA., 67.
- Kloppenborg, B. K., Pieri, R., Eggenstein, H.-B., Maravelias, G., and Pearson, T. 2012. *J. Amer. Assoc. Var. Star Obs.*, **40**, 815.
- Koen, C. 2001, *Mon. Not. Roy. Aston. Soc.*, **321**, 44.
- Loughney, D. 2010, *J. Br. Astron. Assoc.*, **120**, 157.
- Menzies, J. W., Cousins, A. W. J., Banfield, R.M., and Laing, J. D. 1989, *S. Afr. Astron. Obs. Circ.*, **13**, 1.
- Oosterhoff, P. Th. 1966, *Bull. Astron. Inst. Netherlands*, **18**, 140.
- Percy, J. R. 2007, *Understanding Variable Stars*, Cambridge Univ. Press, New York, 62.
- Ponsen, J. 1961, *Bull. Astron. Inst. Netherlands*, **15**, 325.
- Ponsen, J. 1963, *Bull. Astron. Inst. Netherlands*, **17**, 29.
- Richards, T. 2012, *J. Amer. Assoc. Var. Star Obs.*, **40**, 983.
- Vanmuster, T. 2014, Light curve and period analysis software, PERANSO V.2.51 (<http://www.peranso.com/>).
- Walker, S., Butterworth, N., and Pearce, A. 2015, *J. Amer. Assoc. Var. Star Obs.*, **43**, 227.